

# Water mass transformation in the Iceland Sea

Kjetil Våge<sup>a,\*</sup>, G. W. K. Moore<sup>b</sup>, Steingrímur Jónsson<sup>c,d</sup>, and Héðinn Valdimarsson<sup>d</sup>

<sup>a</sup>*Geophysical Institute, University of Bergen and Bjerknes Centre for Climate Research, Bergen, Norway*

<sup>b</sup>*University of Toronto, Toronto, Canada*

<sup>c</sup>*University of Akureyri, Akureyri, Iceland*

<sup>d</sup>*Marine Research Institute, Reykjavik, Iceland*

---

## Abstract

The water mass transformation that takes place in the Iceland Sea during winter is investigated using historical hydrographic data and atmospheric reanalysis fields. Surface densities exceeding  $\sigma_{\theta} = 27.8 \text{ kg/m}^3$ , and hence of sufficient density to contribute to the lower limb of the Atlantic Meridional Overturning Circulation via the overflows across the Greenland-Scotland Ridge, exist throughout the interior Iceland Sea east of the Kolbeinsey Ridge at the end of winter. The deepest and densest mixed layers are found in the north-west Iceland Sea on the outskirts of the basin's cyclonic gyre, largely determined by stronger atmospheric forcing near the ice edge. Much of the accumulated wintertime heat loss in that region takes place during a few extreme cold air outbreak events. Only a small number of hydrographic profiles (2%) recorded mixed layers sufficiently dense to supply the deepest part of the North Icelandic Jet, a current along the slope off northern Iceland that advects overflow water into the Denmark Strait. However, low values of potential vorticity at depth indicate that waters of this density class may be ventilated more regularly than the direct observations of dense mixed layers in the sparse data set indicate. A sudden increase in the depth of this deep isopycnal around 1995 suggests that the supply of dense water to the North Icelandic Jet, and hence to the densest component of the Atlantic Meridional Overturning Circulation, may have diminished over the past 20 years. Concurrent reductions in the turbulent heat fluxes and wind stress curl over the Iceland Sea are consistent with a decrease in convective activity and a weakening of the cyclonic gyre, both of which could have caused the increase in depth of these dense waters.

**Keywords:** Iceland Sea, Open-ocean convection, North Icelandic Jet, Denmark Strait Overflow Water, Atlantic Meridional Overturning Circulation, Cold air outbreak, Icelandic Low, Lofoten Low, North Atlantic Oscillation

---

\*Corresponding author.

Email address: kjetil.vage@gfi.uib.no (Kjetil Våge)

27 **1. Introduction**

28 The water mass transformation that takes place within the Nordic Seas, at the northern extrem-  
29 ity of the Atlantic Meridional Overturning Circulation (AMOC), impacts the world ocean and is  
30 of key importance for the North Atlantic climate system (e.g. Gebbie and Huybers, 2010; Rhines  
31 et al., 2008). Warm, saline Atlantic waters flow northward across the Greenland-Scotland Ridge  
32 into the Nordic Seas, release heat to the atmosphere, and the resulting densified waters return  
33 southward through gaps in the ridge as overflow plumes. While the overflow transport is about  
34 evenly divided east and west of Iceland, the largest overflow plume and the densest contribution  
35 to the lower limb of the AMOC passes through the Denmark Strait between Greenland and Ice-  
36 land (Fig. 1, Jochumsen et al., 2013).

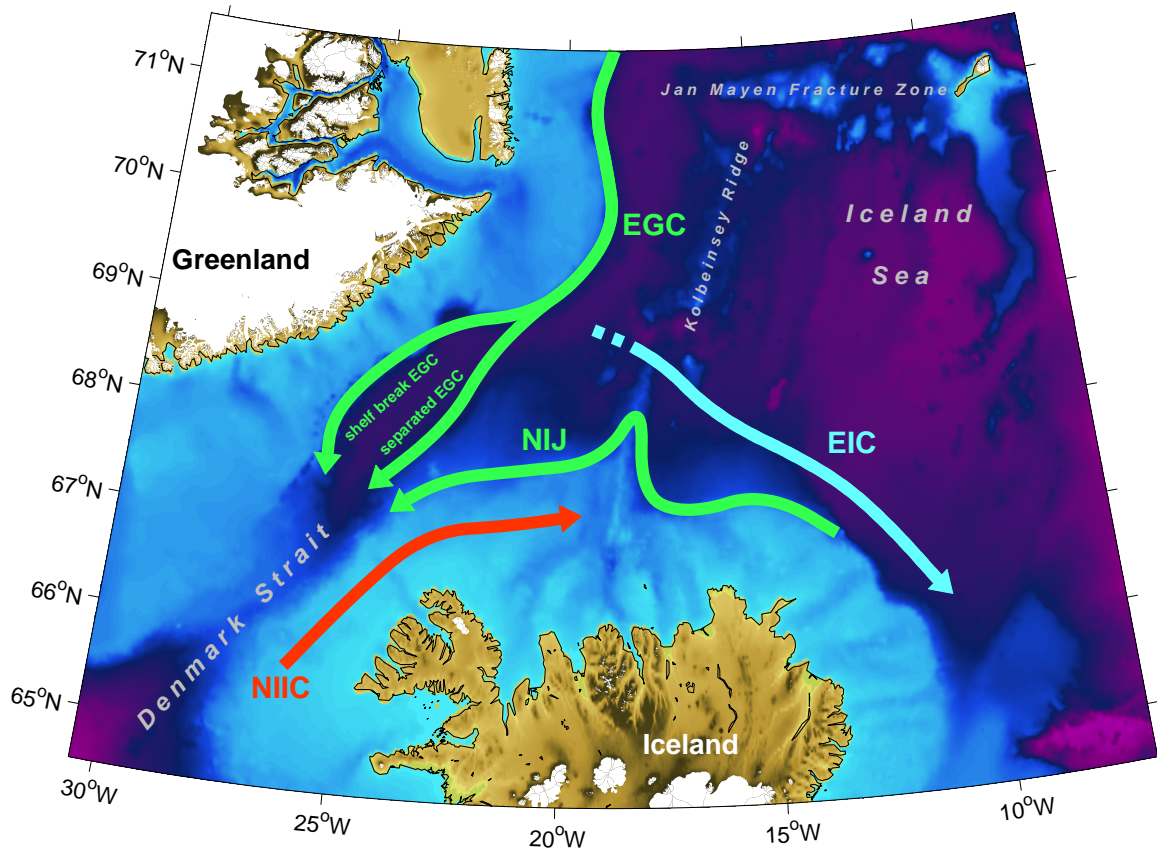


Figure 1: Bathymetry and schematic circulation in the Iceland Sea. The acronyms are: EGC = East Greenland Current; NIJ = North Icelandic Jet; EIC = East Icelandic Current; NIIC = North Icelandic Irminger Current.

37 The winter mean climate of the subpolar North Atlantic is dominated by a large-scale pressure  
38 dipole known as the North Atlantic Oscillation (NAO) with the Icelandic Low and Azores High

39 being its centers of action (Hurrell, 1995; Hurrell and Deser, 2009). The NAO is considered to be  
40 in its positive state when the sea level pressure is anomalously high (low) in the southern (northern)  
41 center of action. In its positive state, there is enhanced westerly flow across the mid-latitudes of  
42 the North Atlantic. The Iceland Sea is situated in the trailing trough that extends northeastwards  
43 from the Icelandic Low towards the Barents Sea (Serreze et al., 1997). Along this trough there  
44 is a secondary low-pressure center known as the Lofoten Low that has a climatological center to  
45 the west of northern Norway near 72°N, 14°E (Jahnke-Bornemann and Bruemmer, 2009). The  
46 pressure dipole consisting of the Icelandic and Lofoten Lows is known as the Icelandic Lofoten  
47 Dipole (ILD). In addition to being important features in the winter mean flow, these two locations  
48 are also the primary (Icelandic Low) and secondary (Lofoten Low) maxima in cyclone frequency  
49 over the subpolar North Atlantic (Wernli and Schwierz, 2006). Although the NAO and ILD share  
50 a common center of action, the Icelandic Low, Jahnke-Bornemann and Bruemmer (2009) have  
51 shown that since the 1980s the two pressure dipoles are only weakly correlated.

52 The winter mean atmospheric circulation over the subpolar North Atlantic is therefore the  
53 result of a complex interplay between these two quasi-independent pressure dipoles. With regard  
54 to the Iceland Sea, it appears that the ILD is the primary mode of inter-annual variability (Kelly  
55 et al., 1987; Jahnke-Bornemann and Bruemmer, 2009; Moore et al., 2012, 2014). During periods  
56 when the Icelandic Low is anomalously deep, southerly flow is established over the Iceland Sea  
57 resulting in the advection of warm air and a concomitant reduction in the magnitude of the air-sea  
58 heat fluxes (Moore et al., 2012). In contrast, when the Lofoten Low is anomalously deep, the  
59 Iceland Sea is under the influence of northerly flow that advects cold air into the region leading  
60 to an increase in the magnitude of the sea to air heat fluxes. As a result of this sea-level pressure  
61 distribution, the Iceland Sea is situated in a saddle point between the two lows and this leads to a  
62 local minimum in air-sea total turbulent heat flux (Moore et al., 2012).

63 Despite relatively weak atmospheric forcing, oceanic convection takes place in the central Ice-  
64 land Sea east of the Kolbeinsey Ridge (Fig. 1) and results in the formation of Arctic Intermediate  
65 Water (Swift and Aagaard, 1981). Doming isopycnals associated with the presence of a cyclonic  
66 gyre (Stefánsson, 1962; Swift and Aagaard, 1981; Voet et al., 2010) facilitate the water mass trans-  
67 formation. Typical late-winter mixed-layer depths are on the order of 200 m (Swift and Aagaard,  
68 1981). The remnants of this convective product are observed during the rest of the year as a cold  
69 layer near this depth (e.g. Jónsson, 2007).

70 The depth of convection in the Iceland Sea is to some extent regulated by the magnitude of  
71 the wind stress curl, which has a pronounced influence on the surface salinity (Jónsson, 1992).

72 Fresh conditions during the so-called “ice years” of the late 1960s may have caused a temporary  
73 cessation of convection (Malmberg and Jónsson, 1997). At that time the East Icelandic Current,  
74 usually an ice free current, transported a larger amount of cold, fresh water of polar origin as  
75 well as a substantial amount of drift ice, perhaps brought about by a period of northerly winds  
76 and reduced wind stress curl (Dickson et al., 1975; Jónsson, 1992). Over the past three decades a  
77 pronounced decline in sea ice concentration in the western Nordic Seas has led to a retreat of the  
78 ice edge from the cyclonic gyre in the central Iceland Sea. Simulations with a one-dimensional  
79 mixed-layer model predict that the ensuing trend of diminished wintertime atmospheric forcing  
80 will reduce the depth and density of the convective product (Moore et al., 2015).

81 While earlier studies claimed significant contributions from the Iceland Sea to the Denmark  
82 Strait overflow plume (e.g. Swift et al., 1980; Livingston et al., 1985; Smethie Jr. and Swift, 1989),  
83 the current consensus is that the transformation of Atlantic inflow into Denmark Strait Overflow  
84 Water (DSOW) occurs primarily within the cyclonic circulation around the margins of the Nordic  
85 Seas (Mauritzen, 1996; Eldevik et al., 2009). In this scenario interior convection in the western  
86 basins contributes only to a minor extent. It is generally thought that DSOW is mainly advected to  
87 the Denmark Strait by the East Greenland Current (e.g. Rudels et al., 2002), but that it contains to  
88 various extents an admixture of water formed within the Iceland Sea (Olsson et al., 2005; Tanhua  
89 et al., 2005, 2008; Jeansson et al., 2008). The variability among these studies may be related in  
90 part to a temporal switching between sources of DSOW (Rudels et al., 2003; Holfort and Albrecht,  
91 2007; Köhl, 2010).

92 The emphasis on the Iceland Sea as a source of DSOW was renewed with the discovery of a  
93 current flowing along the slope north of Iceland in the direction of the Denmark Strait, later called  
94 the North Icelandic Jet (NIJ), by Jónsson (1999) and Jónsson and Valdimarsson (2004). They  
95 found that the NIJ was potentially of sufficient strength to account for the bulk of the overflow  
96 water if some entrainment of ambient water is assumed. Extensive hydrographic/velocity surveys  
97 along the slope west and north of Iceland indicate that the NIJ advects both the densest overflow  
98 water as well as a major fraction of the total overflow transport (1.4-1.5 Sv, 1 Sv =  $10^6$  m<sup>3</sup>/s) into  
99 the Denmark Strait (Våge et al., 2011, 2013). Observations and numerical simulations suggest  
100 that the NIJ originates along the northern coast of Iceland (Våge et al., 2011; Logemann et al.,  
101 2013; Yang and Pratt, 2014). In particular, Våge et al. (2011) hypothesize that it is the deep limb  
102 of an overturning loop that involves the boundary current system north of Iceland and water mass  
103 transformation in the central Iceland Sea.

104 Several studies indicate that waters ventilated in the Iceland Sea also take part in the overflows

105 east of Iceland. The Faroe Bank Channel overflow contains a small contribution from the Iceland  
106 Sea in the form of Modified East Icelandic Water (Meincke, 1978; Hansen and Østerhus, 2000;  
107 Fogelqvist et al., 2003). Perkins et al. (1998) found at least 0.7 Sv of Arctic Intermediate Water  
108 primarily originating from the Iceland Sea to participate in the overflow through the gap in the  
109 ridge east of Iceland. There are additional sporadic overflows through other notches along the  
110 Iceland-Faroe Ridge that likely contain some water originating from the Iceland Sea (Meincke,  
111 1983). In total the overflow of water ventilated in the Iceland Sea across the Iceland-Scotland  
112 Ridge could amount to 0.5-1 Sv, which is consistent with the fluxes of Arctic waters from the  
113 Iceland Sea toward the east reported by Jónsson (2007).

114 The potential contribution from the Iceland Sea to the ventilation of the world ocean via over-  
115 flows across the Greenland-Scotland Ridge could then be on the order of 2 Sv. This is a substantial  
116 fraction of the total overflow, which is generally thought to be about 6 Sv (Østerhus et al., 2008).  
117 The motivation for the present study is to shed light on the wintertime water mass transformation  
118 that takes places in the Iceland Sea and supplies densified water to the Nordic Seas' overflows. Us-  
119 ing a collection of historical hydrographic profiles and atmospheric reanalysis fields we investigate  
120 the coupled ocean-atmosphere system in the Iceland Sea region. In particular, we show that waters  
121 of sufficient density to contribute to the overflows are produced throughout the central Iceland Sea,  
122 investigate the extent to which the densest water masses that are transported by the NIJ and feed  
123 the DSOW plume may be formed in this region, and link a decrease in the supply of this dense  
124 water to diminishing levels of atmospheric forcing.

## 125 **2. Data and methods**

126 The historical hydrographic data set used in this study is a new version of that employed by  
127 Våge et al. (2013) updated to include the most recent profiles. The data set covers the period 1980  
128 to present and was compiled from various data bases and the Argo global program of profiling  
129 floats. Prior to the first deployment of Argo floats in the Iceland Sea in October 2005, the central  
130 and northern Iceland Sea was, in particular during winter, sparsely sampled. Additional details  
131 about the data set, its quality control, and the gridding procedure can be found in Våge et al.  
132 (2013).

133 In order to determine mixed-layer depths, each of the hydrographic profiles in the historical  
134 data set was visually inspected. Two automated routines were employed to identify the base of  
135 the mixed layer. The difference criterion method used by Nilsen and Falck (2006) to investigate  
136 mixed-layer properties in the Norwegian Sea was adapted to the more weakly stratified conditions

137 in the Iceland Sea. In particular, the potential density near the base of the mixed layer was estimated  
138 from the surface properties by subtracting  $\Delta T = 0.2^\circ\text{C}$  (Nilsen and Falck, 2006, used a temperature  
139 difference of  $\Delta T = 0.8^\circ\text{C}$ ). By contrast, the method of Lorbacher et al. (2006) identified the base  
140 of the mixed layer as the shallowest extreme in curvature of the temperature profile. For more  
141 than half (56%) of the profiles the mixed-layer depth was adequately determined by one or both  
142 of these automated routines as judged by visual inspection. The routines performed particularly  
143 well on summer and early fall profiles, when the upper ocean was more stratified and there was  
144 a pronounced density difference between the base of the mixed layer and the lower part of the  
145 profile, but were less accurate during periods of active convection that eroded the stratification.  
146 The automated routines were also unable to identify mixed layers isolated from the surface, either  
147 in the form of multiple vertically stacked mixed layers or as early stages of restratification, both of  
148 which are prevalent also in the Labrador and Irminger Seas during winter (Pickart et al., 2002; Våge  
149 et al., 2011). For these remaining profiles (44%) the mixed-layer depth was determined manually  
150 following a robust method developed by Pickart et al. (2002) that involves a visual estimation of  
151 the mixed-layer extent and the location(s) where the profile permanently crossed outside a two-  
152 standard deviation envelope calculated over that depth range.

153 The atmospheric reanalysis product employed in this study is the global Interim Reanalysis  
154 (ERA-I) from the European Centre for Medium Range Weather Forecasts (Dee et al., 2011). We  
155 use the  $0.75^\circ$  6-hourly fields of sea-level pressure, 10 m winds, sea ice, and the turbulent and  
156 momentum fluxes for the period from January 1979 to April 2013. Comparison with aircraft and  
157 ship observations in the southeast Greenland region show good agreement with ERA-I (Renfrew  
158 et al., 2009; Harden et al., 2011).

159 The statistical significance of changes in the appearance of time series of interest, such as a  
160 linear trend or a transition in mean behavior across a given temporal breakpoint, was assessed  
161 using a Monte Carlo significance test that takes into account the temporal auto-correlation charac-  
162 teristics of geophysical time series (Rudnick and Davis, 2003; Moore, 2012). Specifically, 10000  
163 synthetic time series were generated that shared the same spectral characteristics as the time series  
164 in question. These synthetic time series were then used to estimate the probability distribution for  
165 the given change in behavior thereby allowing one to estimate the statistical significance of this  
166 change in the underlying time series.

### 167 3. Wintertime convection in the Iceland Sea

168 Maps of near-surface wintertime hydrographic properties in the Iceland Sea were first presented  
169 by Swift and Aagaard (1981) based on a ship-board survey that took place in late February/early  
170 March 1975. They found water denser than  $\sigma_\theta = 27.8 \text{ kg/m}^3$ , which is typically used to delimit  
171 overflow water (e.g. Dickson and Brown, 1994), throughout most of the central Iceland Sea. The  
172 densest mixed layers were located in the northern part of the Iceland Sea. Our late winter (February  
173 through April) mixed-layer potential densities (Fig. 2a) are slightly lower in the southern part of  
174 the Iceland Sea, due to a combination of fresher and warmer waters, but otherwise in qualitative  
175 agreement with Swift and Aagaard's (1981) near-surface densities. The corresponding map of  
176 mixed-layer depths (Fig. 2b) shows that also the deepest mixed layers tend to be found in the  
177 northern Iceland Sea. Mixed layers shallower than 25 m, due to early stages of restratification,  
178 were disregarded. While the data nominally span a temporal range of 1980 to present, wintertime  
179 observations from the interior Iceland Sea were scarce prior to the deployment of the first Argo  
180 floats in late 2005. Most (67%) of the data from the north-central Iceland Sea area outlined in  
181 Fig. 2 stem from the period 2005 to present.

182 It is interesting to note that the deepest and densest mixed layers are found on the outskirts of  
183 the Iceland Sea Gyre (Fig. 2). Open ocean convection is normally thought to take place within  
184 cyclonic gyres (e.g. Marshall and Schott, 1999). Doming isopycnals within a gyre bring weakly  
185 stratified water closer to the surface resulting in a water column that is more preconditioned for  
186 convection (Fig. 3a illustrates that this is the case also in the Iceland Sea). As winter sets in,  
187 increased buoyancy loss erodes the near-surface stratification and exposes the weakly stratified  
188 water beneath directly to the atmospheric forcing, which allows deeper convection to commence.  
189 Off the center of a gyre the water column is less preconditioned, typically resulting in reduced  
190 convective activity. We will demonstrate in Section 6 that stronger atmospheric forcing in the  
191 northern part of the Iceland Sea is primarily responsible for the deeper and denser mixed layers  
192 there, on the outskirts of the gyre.

193 More intense convection off the center may alter the density structure of the gyre and thereby  
194 also its circulation. However, the main seasonal signal in dynamic height of the surface relative  
195 to a deep reference level was a near-uniform increase in summer (not shown). This is primarily  
196 caused by a change in steric height due to thermal expansion. The center position and shape of  
197 the gyre were qualitatively similar between the different seasons. These results are in accordance  
198 with Voet et al. (2010), who found a very weak seasonal signal in the circulation of the Iceland Sea  
199 Gyre.

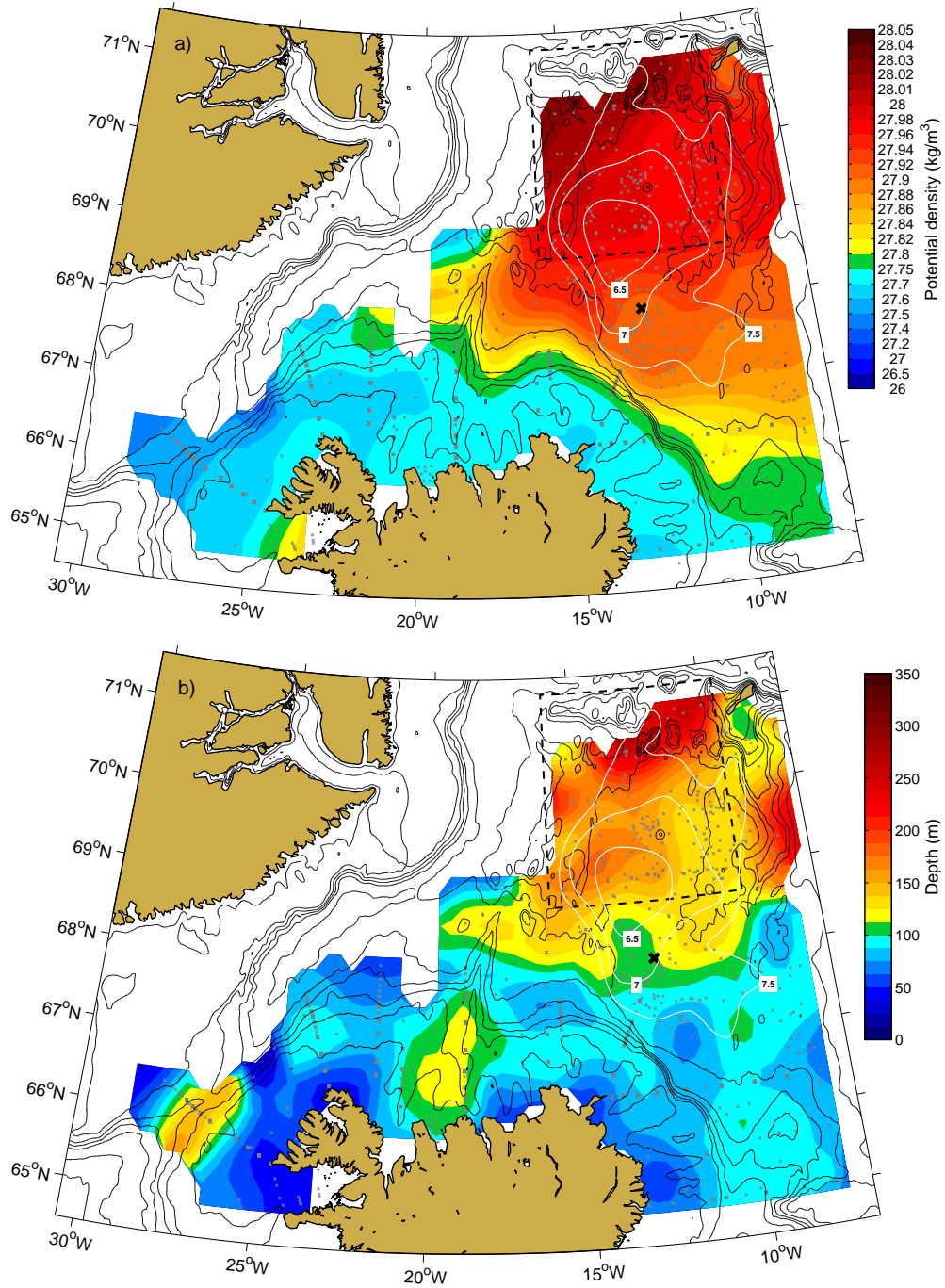


Figure 2: Late-winter (Feb-Apr) mixed-layer potential density (a) and depth (b). The north-central Iceland Sea is outlined by the black dashed lines and the white lines are summer (May through October) contours of dynamic height of the surface relative to 500 db in units of dynamic cm (Våge et al., 2013). The gray crosses mark the locations of data points and the black cross represents the Langanes 6 repeat hydrographic station. The 200 m, 400 m, 600 m, 800 m, 1000 m, 1400 m, and 2000 m isobaths are contoured as black lines.



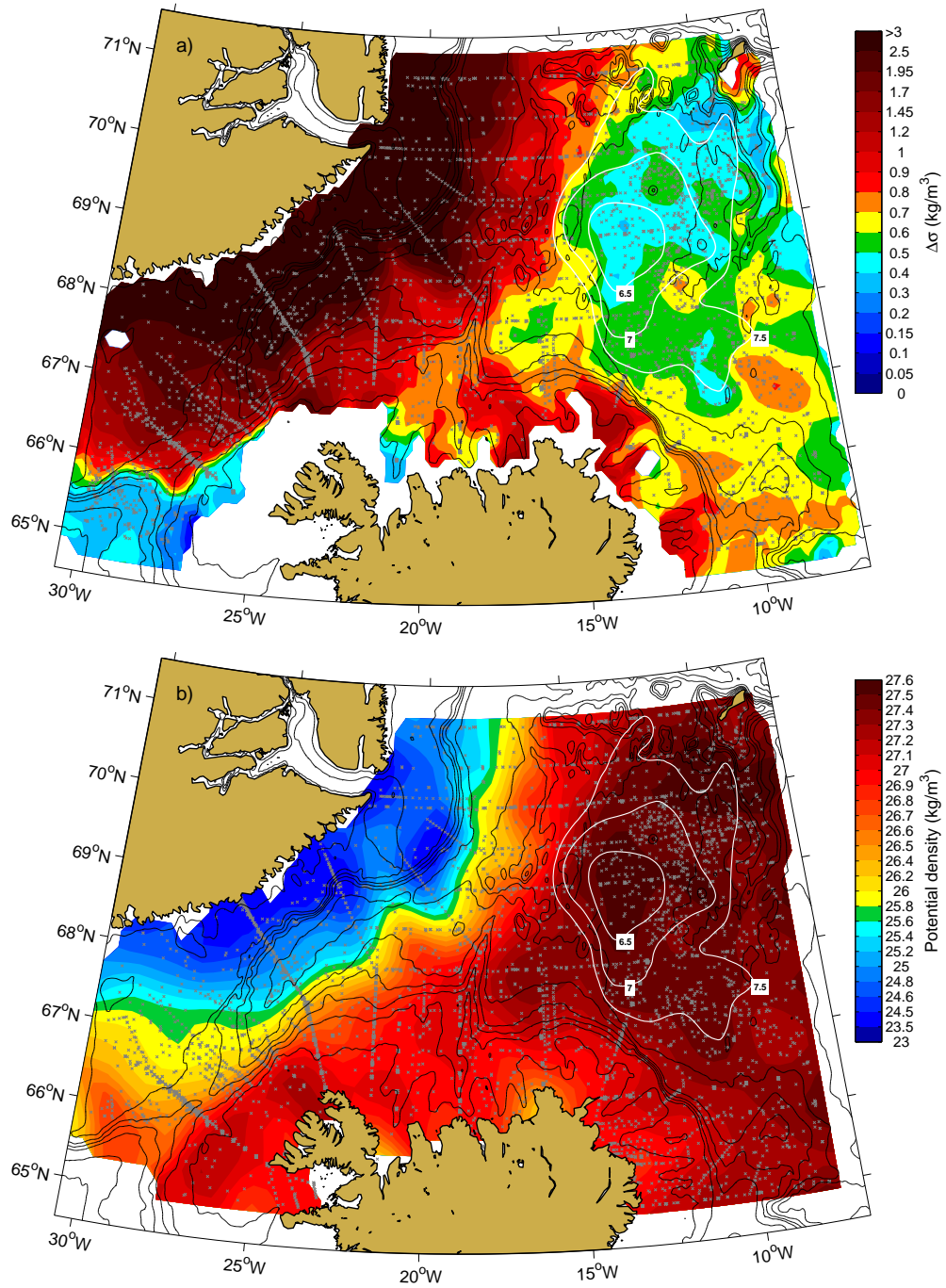


Figure 3: Summer half-year (May-Oct) stratification (a, as the difference in potential density between 10 and 250 m) and potential density in the mixed layer (b). The white lines are contours of dynamic height of the surface relative to 500 db in units of dynamic cm (Våge et al., 2013), and the gray crosses mark the locations of data points. The 200 m, 400 m, 600 m, 800 m, 1000 m, 1400 m, and 2000 m isobaths are contoured as black lines.

#### 200 4. Mixed-layer evolution in the north-central Iceland Sea

201 The densest and deepest late-winter mixed layers were recorded in the north-central part of  
202 the Iceland Sea (the area enclosed by the black dashed line in Fig. 2, which also contains the  
203 northern half of the gyre). To better understand the seasonal evolution of the upper part of the  
204 water column that actively takes part in wintertime convection, we examined the month-to-month  
205 change in mixed-layer properties in this region. During more than half of the year, from November  
206 through May, the potential density of the mixed layer exceeded  $\sigma_\theta = 27.8 \text{ kg/m}^3$  (Fig. 4a), and  
207 had thereby attained sufficient density to potentially contribute to the overflows from the Nordic  
208 Seas. The mixed-layer potential density and depth monotonically increased from November to  
209 March. While the hydrographic properties were largely uniform at the tail end of winter, the high  
210 variability in mixed-layer depth in April indicates that the onset of restratification tends to take  
211 place during that month (Fig. 4b). With abating levels of buoyancy and wind forcing as well as  
212 increasing insolation in spring, wintertime convection comes to a halt and a shallow, warm surface  
213 layer develops.

214 The seasonal evolution of the upper water column is evident also in Fig. 5 by increased near-  
215 surface densities and deeper mixed layers in winter. While there is a trend of increasingly deep  
216 mixed layers during the course of each winter, it is clearly not as monotonic as suggested by  
217 Fig. 4b. This is due to the non-uniform spatial and temporal character of convection. In particular,  
218 mixed layers near the northern end of the domain were in general deeper than those farther south.  
219 Inter-annual variability in mixed-layer depth and potential density is clearly present as well. This  
220 is dominated by changes in the magnitude of the atmospheric forcing, but the stratification of the  
221 upper water column prior to the onset of wintertime convection also plays a role.

222 The mixed-layer evolution documented in Figs. 4 and 5 suggests that the  $\sigma_\theta = 28.03 \text{ kg/m}^3$   
223 isopycnal is only on occasion ventilated in the Iceland Sea. In fact, only five of the late-winter  
224 profiles contained mixed layers with greater potential density, all of which came from Argo floats  
225 in the northern Iceland Sea in winter 2013. Våge et al. (2011) found that a substantial portion of the  
226 NIJ transport ( $0.6 \pm 0.1 \text{ Sv}$ ) was of a density class exceeding  $\sigma_\theta = 28.03 \text{ kg/m}^3$  and hypothesized  
227 that it was fed by waters originating from overturning in the interior Iceland Sea. This begs the  
228 question: to what extent does the Iceland Sea provide the densest contribution to the NIJ and hence  
229 to the Denmark Strait overflow plume?

230 Data from one particular Argo float, documented for more than two years and corrected for  
231 drift in the conductivity and pressure sensors (Wong et al., 2003), may indicate that ventilation  
232 of waters denser than  $\sigma_\theta = 28.03 \text{ kg/m}^3$  is more prevalent than the few direct records of such

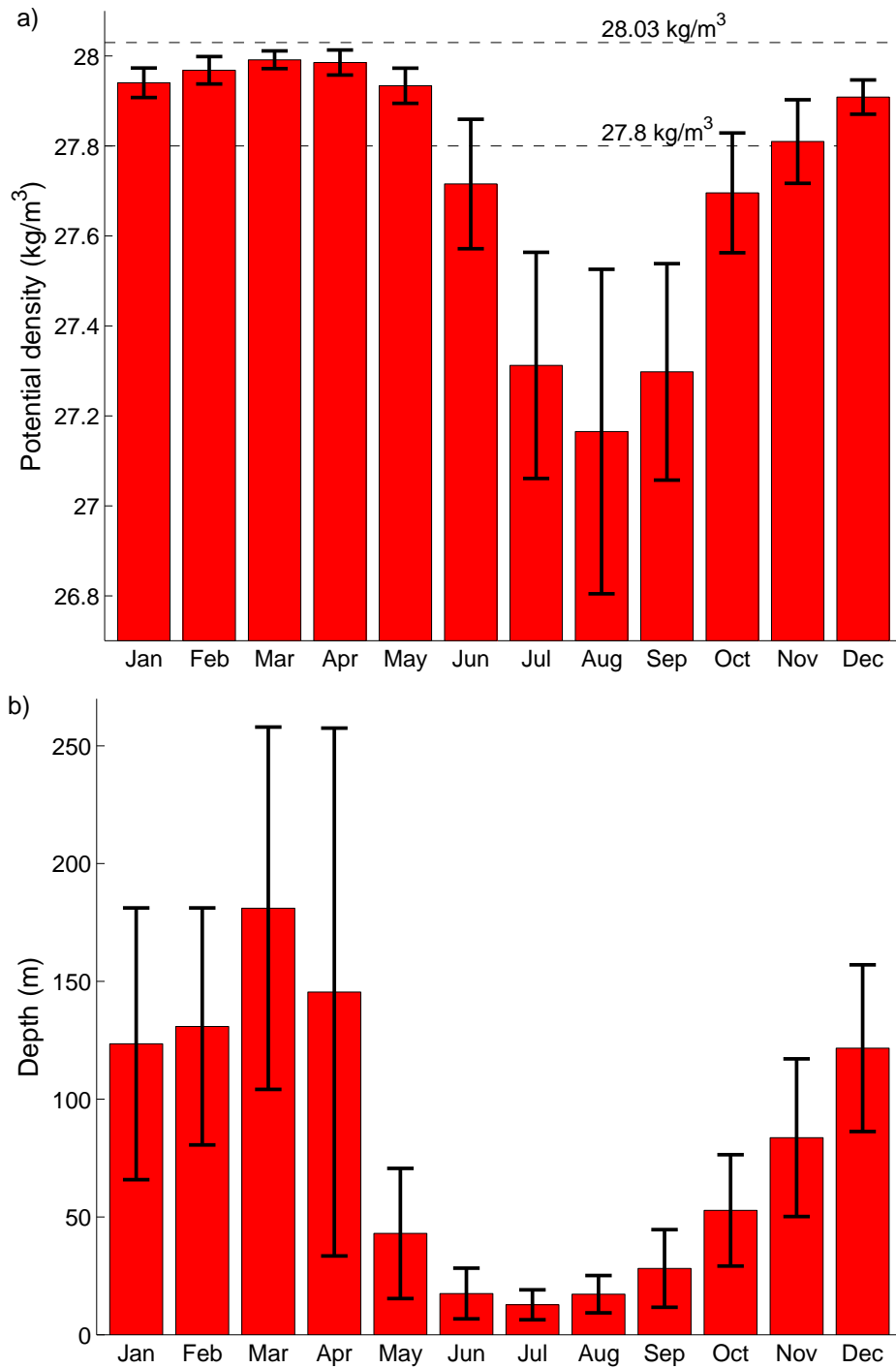


Figure 4: Seasonal evolution of the mixed-layer potential density (a) and depth (b) within the north-central Iceland Sea area indicated in Fig. 2. The red bars and the vertical black lines represent the monthly means and standard deviations, respectively. (With sample sizes ranging from 41 in January to 190 in August, the standard error of the mean is very small for most months.)

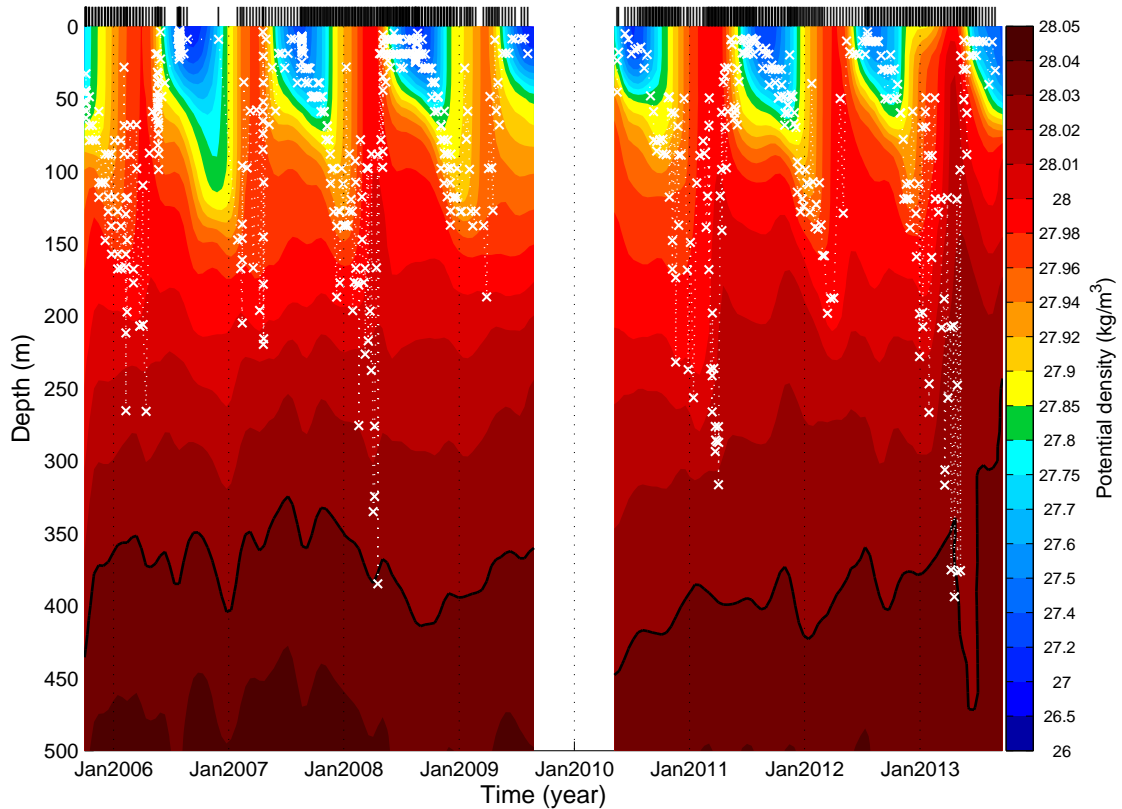


Figure 5: Temporal evolution of potential density in the upper 500 m within the north-central Iceland Sea area indicated in Fig. 2. Each profile, denoted by a vertical bar along the top, is considered representative of this region. The white crosses indicate mixed-layer depths. The black contour is the  $\sigma_\theta = 28.03 \text{ kg/m}^3$  isopycnal.

233 dense mixed layers would suggest. The low values of potential vorticity in the upper water col-  
 234 umn in Fig. 6 indicate weak stratification associated with wintertime convection (e.g. Talley and  
 235 McCartney, 1982). During its trajectory through the northern Iceland Sea in winter 2007-2008,  
 236 the float encountered mixed layers deeper than 300 m (isolated from the surface by early stages  
 237 of restratification, but clearly formed during the same winter, see for example Våge et al., 2009).  
 238 While neither this float nor any of the other profiles from winter 2007-2008 recorded mixed-layers  
 239 denser than  $\sigma_\theta = 28.03 \text{ kg/m}^3$ , the lens of weakly stratified water that was present for most of 2008  
 240 between 300 and 450 m and resulted from convection during that winter contained water that ex-  
 241 ceeded this density. This would imply that also waters that may feed the densest portion of the NIJ  
 242 were ventilated in the Iceland Sea in winter 2007-2008. Indeed, a substantial number of the north-  
 243 central Iceland Sea profiles (about 6%) had a potential vorticity of less than  $8 \text{ (ms)}^{-1} \times 10^{-12}$  at  
 244 the  $\sigma_\theta = 28.03 \text{ kg/m}^3$  isopycnal, implying that water of this density class may be ventilated on a

245 more regular basis than the direct observations suggest.

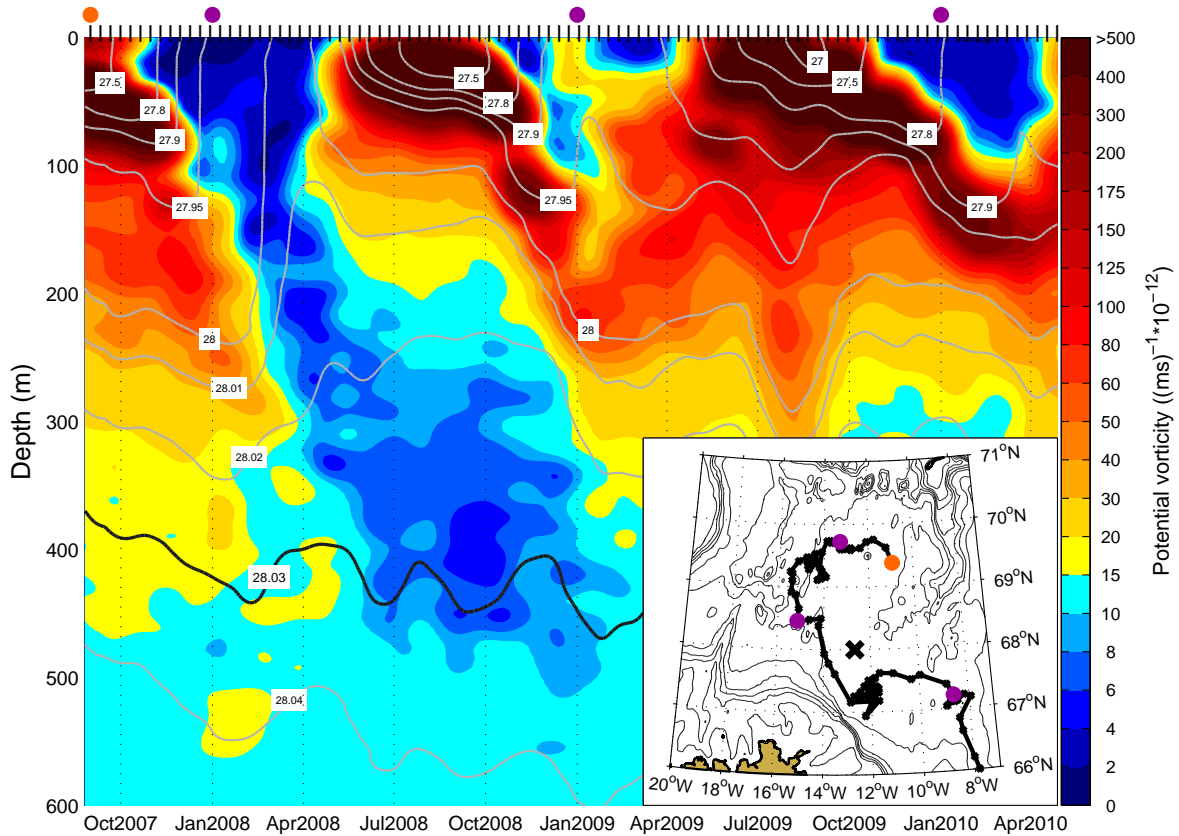


Figure 6: Temporal evolution of potential vorticity (color,  $(\text{ms})^{-1} \times 10^{-12}$ ) and potential density (contours,  $\text{kg/m}^3$ ) along the trajectory of Argo float 7900177 in the Iceland Sea. The vertical bars along the top denote the time of each profile. The inset shows the trajectory of the float. The orange and purple dots mark the float's deployment position and location at the beginning of each January, respectively, and the black cross represents the Langanes 6 repeat hydrographic station. The 200 m, 400 m, 600 m, 800 m, 1000 m, 1400 m, and 2000 m isobaths are contoured as black lines.

## 246 5. Change in availability of dense water to the NIJ during the mid-1990s

247 The sparse amount of wintertime data prior to 2005 in the north-central Iceland Sea precludes  
 248 a thorough investigation into the long-term variability in the ventilation of the densest waters trans-  
 249 ported by the NIJ. We examine instead the depth of the  $\sigma_\theta = 28.03 \text{ kg/m}^3$  isopycnal in the vicinity  
 250 of the outermost station on the Langanes section off the north-east corner of Iceland (Langanes

251 6, black cross in Fig. 2) to shed light on the potential Iceland Sea source of dense water to the  
 252 NIJ. The station is located within the southern part of the gyre, outside the region of most intense  
 253 convection, and is typically sampled four times per year. It is very unlikely that this isopycnal  
 254 was ventilated locally as there were no observed mixed layers with a potential density exceeding  
 255  $27.97 \text{ kg/m}^3$  and the  $\sigma_\theta = 28.03 \text{ kg/m}^3$  isopycnal was not found at shallower depths than 250 m  
 256 over the recorded period (Fig. 7).

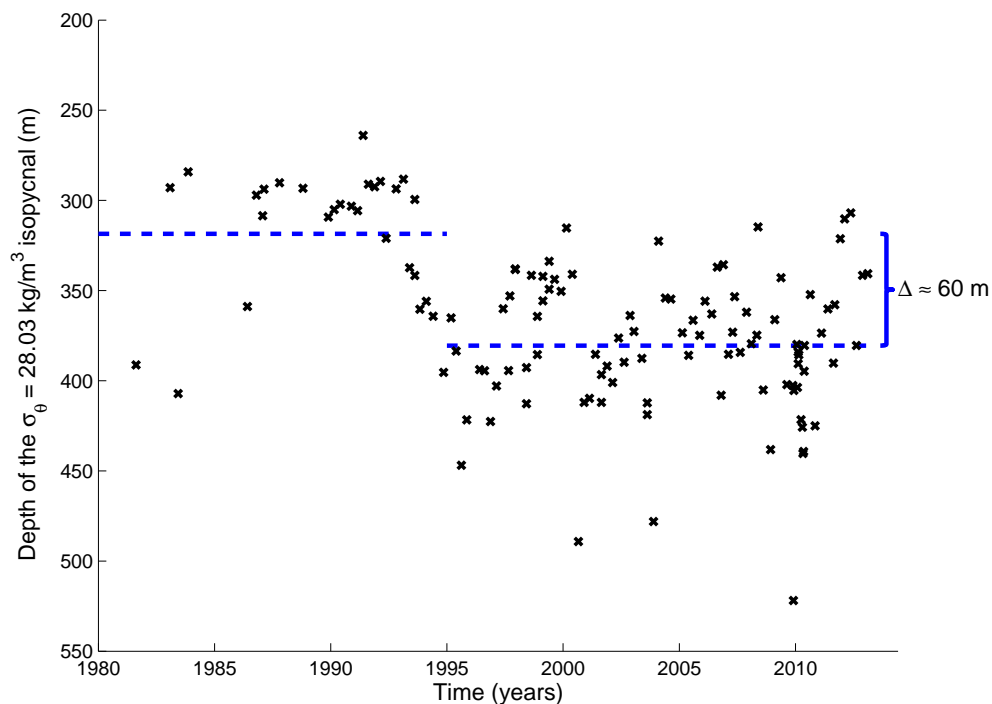


Figure 7: Depth of the  $\sigma_\theta = 28.03 \text{ kg/m}^3$  isopycnal in the vicinity of the repeat station Langanes 6 indicated by the black cross in Fig. 2. The gray lines represent the means of the periods 1980-1995 and 1995-present.

257 The time series of isopycnal depth shown in Fig. 7 indicates that dense water was found higher  
 258 in the water column at the beginning of the record and deeper toward the end. In particular,  
 259 it appears that an abrupt change took place over only 2-3 years around the mid-1990s. Prior  
 260 to 1995 the mean depth of the  $\sigma_\theta = 28.03 \text{ kg/m}^3$  isopycnal was approximately 60 m shallower  
 261 than the following years. Such piecewise constant fits separated by a jump discontinuity across  
 262  $1995 \pm 1$  year were statistically significant with confidence intervals exceeding the 99<sup>th</sup> percentile.  
 263 This may be the result of a change in the convective activity in the Iceland Sea, a persistent change  
 264 in the circulation of the Iceland Sea Gyre, or some combination of both, and has implications for  
 265 the available supply of dense water to the NIJ.

## 266 **6. Atmospheric forcing**

267 In the early 1970s the NAO began a period that was characterized by a positive trend, i.e. a  
268 period during which there was a tendency for enhanced westerlies across the North Atlantic (Hur-  
269 rell, 1995). This period persisted until the early 1990s, when the NAO entered a period where  
270 the trend became negative (Cohen and Barlow, 2005). The winters of 1994-1995 and 1995-1996  
271 marked a particularly dramatic transition from a large positive NAO state to a large negative NAO  
272 state (Fig. 8a, Flatau et al., 2003). However, Cohen and Barlow (2005) note that the statistical sig-  
273 nificance of the trend of the NAO during both periods is generally not robust and highly dependent  
274 on the choice of start and end date. Fig. 8a also shows the linear least squares fit to the winter mean  
275 NAO index. The trend over the entire period is not statistically significant and, in agreement with  
276 Cohen and Barlow (2005), the trends before and after 1995 are not robust. In contrast, the tran-  
277 sition in winter mean NAO index before and after 1995 from positive conditions to more neutral  
278 conditions was statistically significant at the 99<sup>th</sup> percentile confidence level using the aforemen-  
279 tioned test that takes into account the temporal auto-correlation of geophysical time series. The  
280 choice of  $1995 \pm 1$  year as a breakpoint resulted in a minimum in the root mean square error of  
281 the fit to the data. Regardless of how one characterizes the changes in NAO, i.e. as a linear trend  
282 or a jump discontinuity, this transition from positive to neutral NAO conditions has had a number  
283 of impacts on the subpolar North Atlantic. These include a reduction in the magnitude of the wind  
284 stress over the Nordic Seas (Flatau et al., 2003) that has resulted in a weakening and warming of  
285 the subpolar gyre (Häkkinen and Rhines, 2004; Straneo and Heimbach, 2013). The impact of vari-  
286 ability in the ILD on these processes has not been investigated. However, for the period from 1980  
287 onwards an index of the ILD computed from the ERA-I indicates a weak negative trend (Fig. 8b),  
288 i.e. the Icelandic Low is becoming shallower at a faster rate than the Lofoten Low. However, the  
289 trend is not statistically significant at the 95<sup>th</sup> percentile confidence interval. The transition across  
290  $1995 \pm 1$  year, on the other hand, is statistically significant at the 95<sup>th</sup> percentile confidence level.

291 The winter mean (November through April) ERA-I sea-level pressure and 10 m wind field for  
292 the periods 1980-1995 and 1996-2013 as well as the difference between the winter means for the  
293 two periods (i.e. the mean over 1996-2014 minus the mean over 1980-1995) across the Nordic Seas  
294 are shown in Fig. 9. The increase in pressure between the two periods is the result of the weakening  
295 of the Icelandic and Lofoten Lows and is consistent with the behavior of both the NAO and the  
296 ILD over this period. The result is a pronounced reduction in the magnitude of the winter mean  
297 10 m winds along the Denmark Strait as well as over the Iceland Sea. The difference between the  
298 two periods is therefore characterized by an anti-cyclonic circulation anomaly across the Iceland

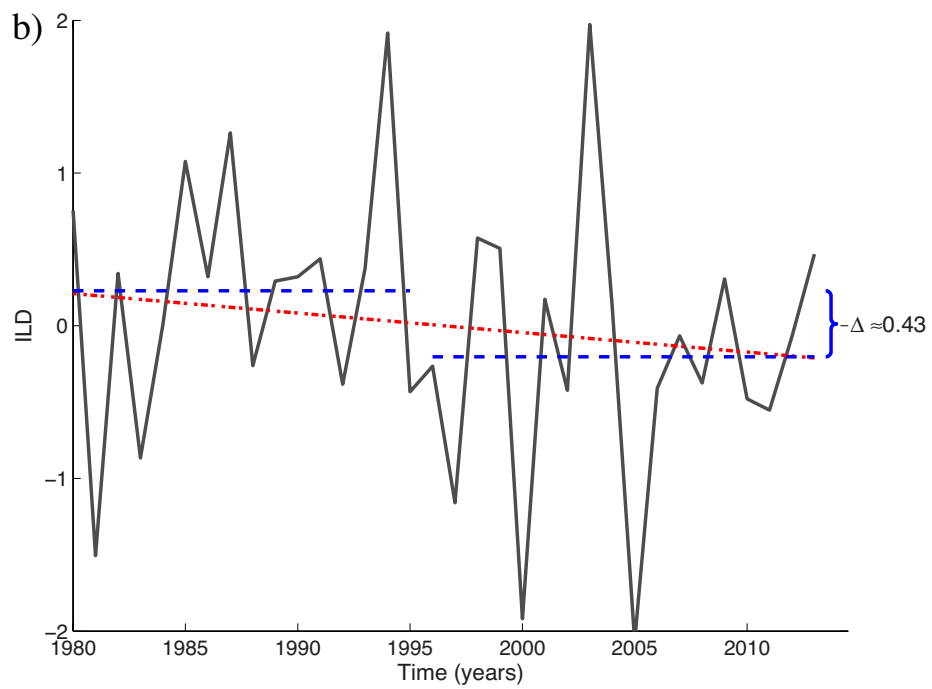
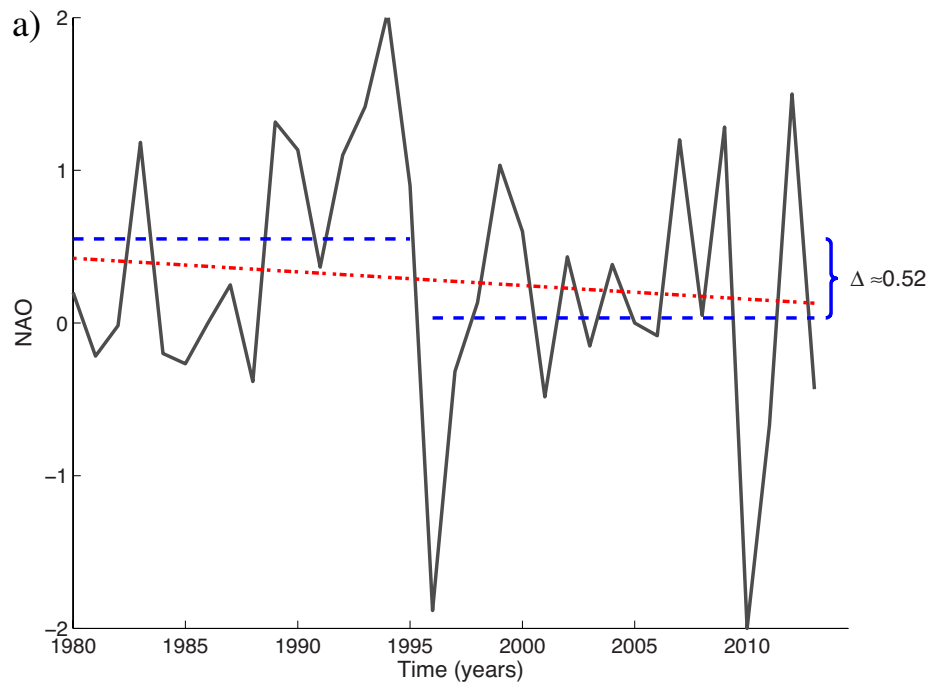


Figure 8: Winter mean NAO (a) and ILD (b) indices. The red dotted lines represent the linear least squares fit to the data, while the blue dashed lines represent mean values before and after a breakpoint during the winter of 1994-1995.



299 Sea.

300 Elevated sea to air heat fluxes over the Iceland Sea (here we will use the convention that heat  
301 fluxes out of the ocean are positive) are associated with strong northerly flow (Moore et al., 2012),  
302 and hence the change in behavior of the atmospheric circulation identified in Fig. 9 should result  
303 in a decrease in the magnitude of the sea to air heat fluxes over the region. Time series of winter  
304 mean turbulent sea to air heat flux, the sum of the sensible and latent heat fluxes, averaged over  
305 the north-central Iceland Sea confirm this decline (Fig. 10a). The curl of the wind stress is positive  
306 over the central Iceland Sea with a narrow band of anti-cyclonic wind stress along the coast that is  
307 the result of lower wind speeds over the sea ice and near coastal regions (Malmberg and Jónsson,  
308 1997; Våge et al., 2013). The wind stress curl also exhibits a considerable amount of inter-annual  
309 variability (Fig. 10b, Malmberg and Jónsson, 1997) that is also most likely regulated by the ILD.  
310 Consistent with Flatau et al. (2003) and Moore et al. (2012), both the winter mean turbulent heat  
311 flux and the wind stress curl have a negative trend, as determined from a linear least squares fit, over  
312 the period 1980-2013. However, only the trend in the turbulent heat flux is statistically significant  
313 at the 95<sup>th</sup> percentile confidence interval (Rudnick and Davis, 2003; Moore, 2012). Also shown in  
314 Fig. 10 are piecewise constant fits to the time series with a breakpoint in 1995. Both time series  
315 can also be characterized by a jump discontinuity across 1995. The statistical significance of the  
316 magnitude of the jump was also considered using an equivalent test. In this case, the magnitude  
317 of jump was statistically significant at the 95<sup>th</sup> percentile confidence interval for both time series.  
318 The root mean square error for the jump discontinuity fit to the data was in both cases smaller than  
319 that for the linear least squares fit, suggesting that the former provides a better fit to the data. The  
320 difference in the characterization of the low frequency variability of the heat flux time series in this  
321 paper with that in Moore et al. (2015) can be attributed to averaging over different spatial regions.

322 The correlations of the winter mean turbulent heat flux and wind stress curl time series with  
323 the corresponding indices of NAO and ILD as well as the sea-level pressures associated with the  
324 Icelandic and Lofoten Lows were calculated. They are generally consistent with the idea that the  
325 Lofoten Low is an important contributor to the variability observed in both time series, with the  
326 Icelandic Low also playing an important role only in the variability observed in the wind stress  
327 curl (Table 1).

328 Moore et al. (2015) attributed the trend in the turbulent heat flux time series to a reduction  
329 in the air-sea temperature difference over the region as well as to a retreat of the sea ice off the  
330 east coast of Greenland. These previous results do not address the changes in the occurrence or  
331 structure of the extreme heat flux events that result in this winter mean behavior. This is important

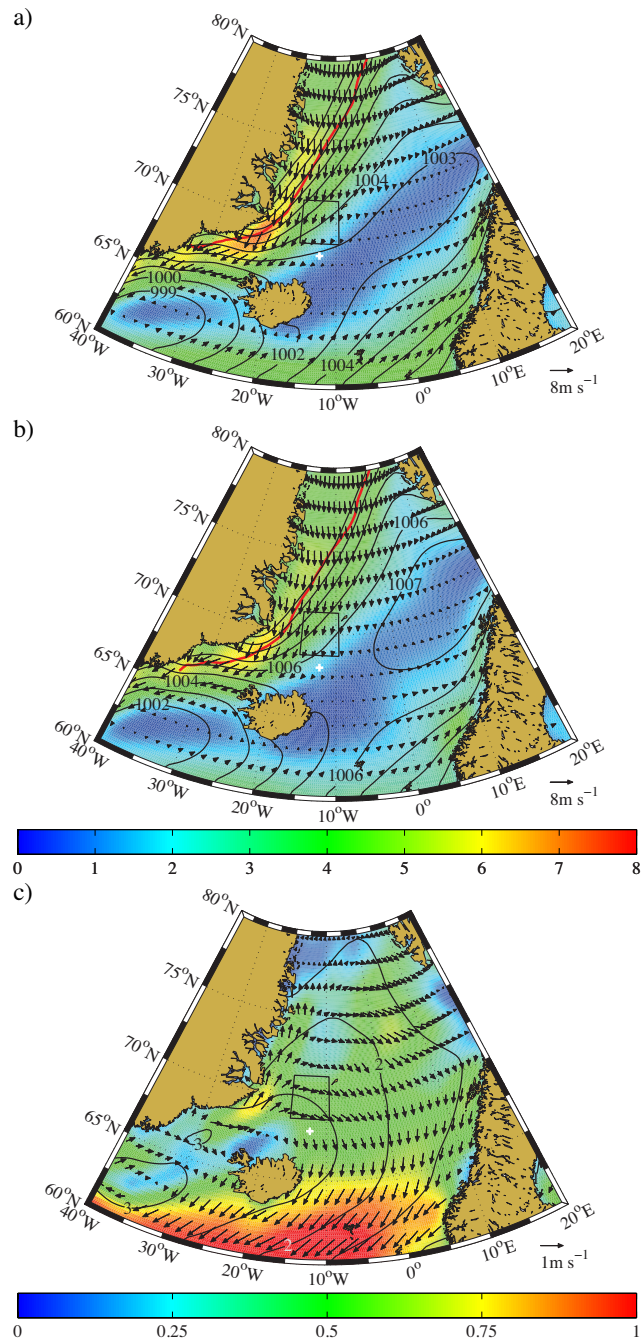


Figure 9: Mean atmospheric circulation over the Nordic Seas during winter (November through April) for the period 1980-1995 (a), the period 1996-2013 (b), and the difference between the periods (i.e. the 1996-2013 mean minus the 1980-1995 mean, c). The sea-level pressure (contours, mb) and 10 m winds (color and vectors, m/s) are shown. The north-central Iceland Sea region is outlined by the black dashed lines and the location of the Langanes 6 station is indicated by the white cross. The thick red curve and (a) and (b) denotes the 50% sea ice concentration contour during the respective period. All data are from the ERA-I reanalysis.

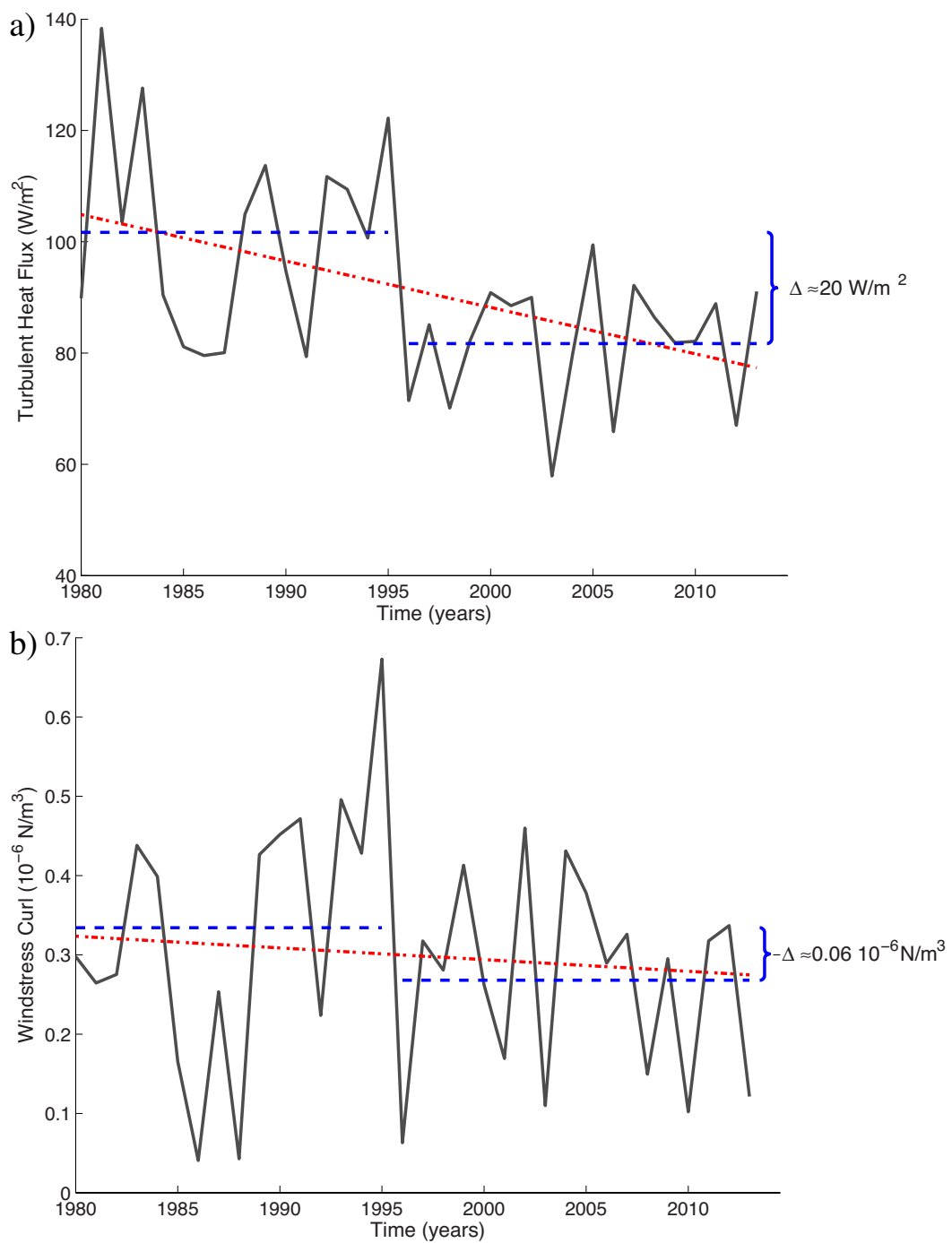


Figure 10: Winter mean total turbulent heat flux (a) and wind stress curl (b) for the north-central Iceland Sea region. The red dotted lines represent the linear least squares fit to the data, while the blue dashed lines represent mean values before and after a breakpoint during the winter of 1994-1995.

	NAO	ILD	Icelandic Low	Lofoten Low
Turbulent heat flux	<u>0.30</u>	<b>-0.37</b>	<u>-0.27</u>	<b>-0.60</b>
Curl of the wind stress	<b>0.63</b>	-0.08	<b>0.60</b>	<b>0.67</b>

Table 1: Correlation coefficients of the winter mean turbulent heat flux and wind stress curl over the north-central Iceland Sea with various indices of the large-scale circulation over the subpolar North Atlantic. Correlations that are underlined are statistically significant at the 95<sup>th</sup> percentile confidence interval, while those that are bold are statistically significant at the 99<sup>th</sup> percentile confidence interval

332 because of the impact that the high heat flux events have on the total loss of heat from the ocean  
333 over a typical winter. For example, events where the turbulent heat flux exceeds the 90<sup>th</sup> percentile  
334 value contribute over 35% of the total winter heat loss. Fig. 11 shows the time series of occur-  
335 rence frequency of extreme turbulent heat fluxes over the north-central Iceland Sea, defined as the  
336 number of times that the turbulent heat flux exceeded the 90<sup>th</sup> or 10<sup>th</sup> percentile value based on all  
337 winter values over the period 1980-2013. These values are 246 and -15 W/m<sup>2</sup>, respectively. The  
338 occurrence of high heat flux events has been decreasing over this period while the occurrence of  
339 events where there was a net warming of the ocean surface have been increasing. This behavior is  
340 consistent with the changes in the winter mean circulation (Fig. 9) which indicate a trend towards  
341 weaker northerly flow into the Iceland Sea since 1980.

342 The sea to air heat fluxes tend to be highest at the ice edge, where the cold and dry Arctic air first  
343 comes in contact with relatively warm surface waters (Marshall et al., 1998; Renfrew and Moore,  
344 1999). As a result, the recent retreat of the sea ice from the vicinity of the Iceland Sea (Strong,  
345 2012; Moore et al., 2015) is also expected to result in a reduction of the magnitude of the sea to air  
346 heat fluxes over the Iceland Sea. To confirm this behavior, all events where the turbulent heat flux  
347 exceeded the 90<sup>th</sup> percentile value, 246 W/m<sup>2</sup>, were identified for the first and last 10 years of the  
348 period of interest, i.e. 1980-1989 and 2004-2013 (Fig. 12). The retreat of the sea ice has resulted  
349 in a northward shift of the region of the largest heat fluxes away from the north-central Iceland Sea  
350 and a narrowing of the marginal ice zone (Strong, 2012). The spatial distribution of the heat fluxes  
351 between the two periods reflects this narrowing. In particular, during the earlier period when the  
352 marginal ice zone was broad, the heat fluxes were significant over a large region, while during the  
353 latter period, characterized by a narrow marginal ice zone, there was a much tighter gradient to the  
354 heat flux. This northward transition of the maximum in the heat fluxes would result in a reduction  
355 in the magnitude of the atmospheric forcing of oceanic convection over the Iceland Sea.

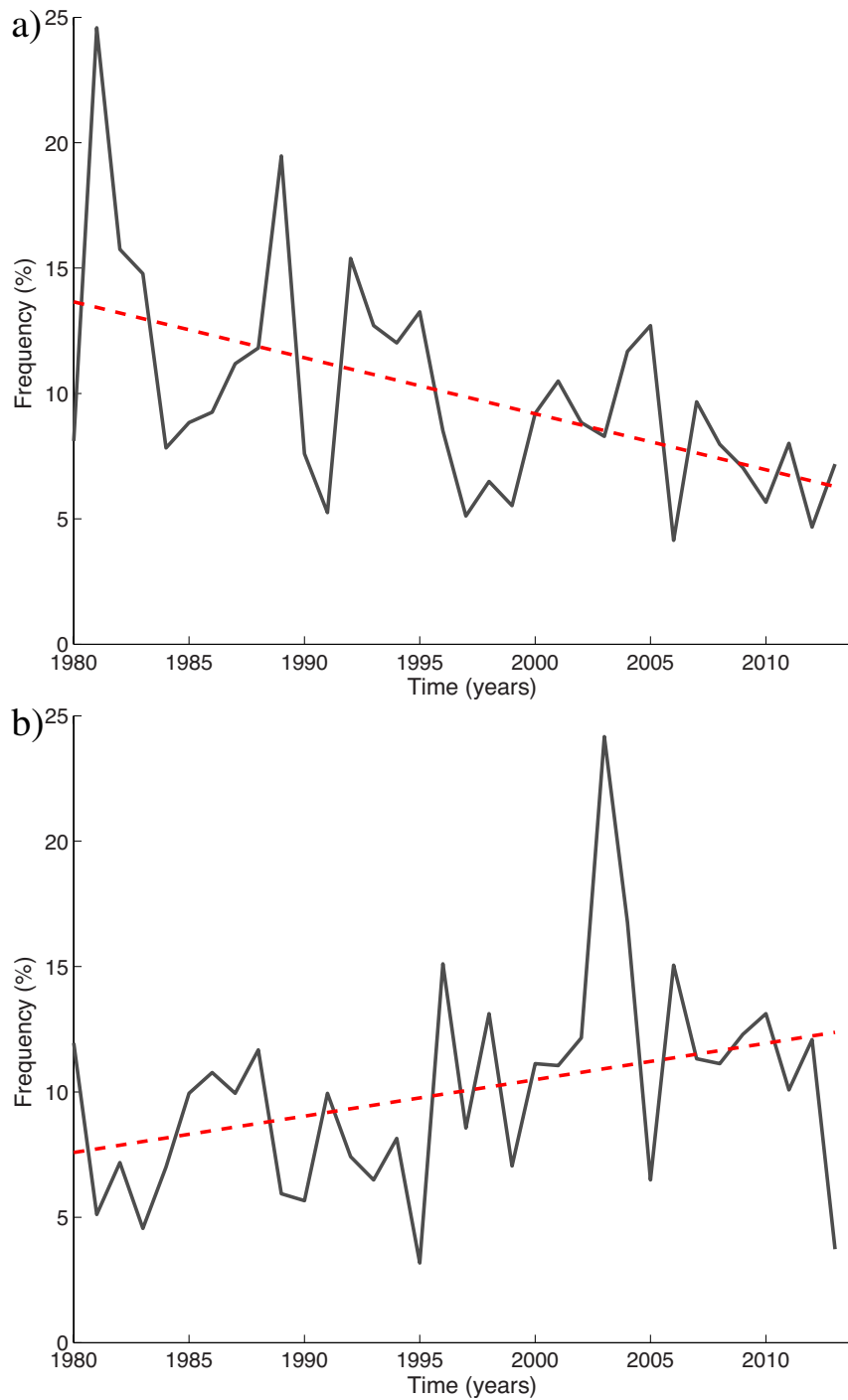


Figure 11: Frequency of occurrence of total turbulent heat fluxes greater than the 90<sup>th</sup> percentile total turbulent heat flux (a) and less than the 10<sup>th</sup> percentile total turbulent heat flux (b) at the middle of the north-central Iceland Sea region.

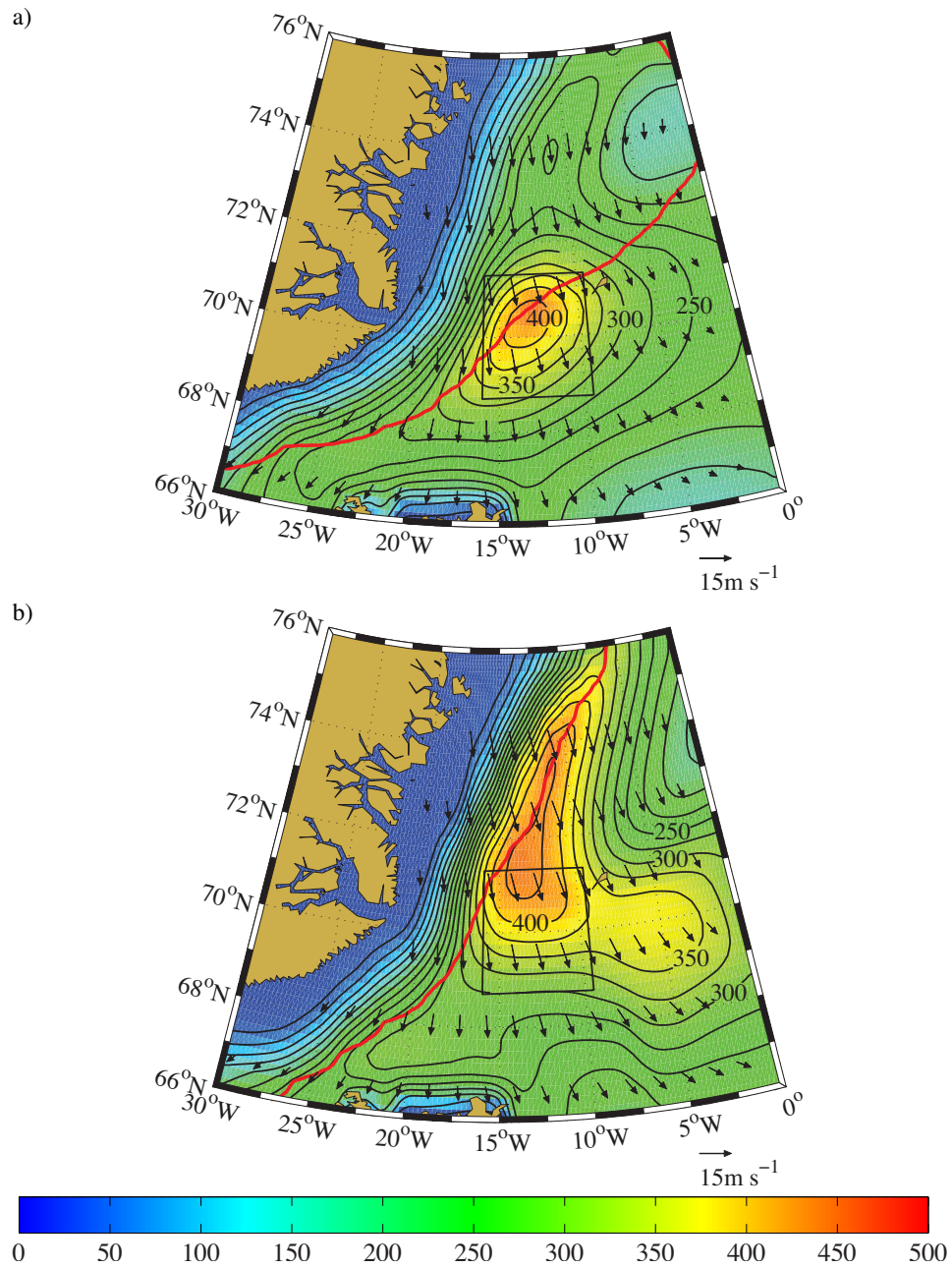


Figure 12: Composite mean high heat flux events at the middle of the north-central Iceland Sea region during 1980-1989 from 75 events (a) and 2004-2013 from 65 events (b). The thick red line represents the composite 50% sea ice concentration contour.

## 356 7. Discussion and conclusions

357 Waters of sufficient potential density to feed the overflows across the Greenland-Scotland  
358 Ridge are formed throughout the Iceland Sea in winter. Its contribution to the overflows could  
359 be on the order of 2 Sv, a considerable fraction of the total overflow of about 6 Sv (Østerhus et al.,  
360 2008). The densest waters are formed in the northern part of the Iceland Sea, on the outskirts of  
361 the cyclonic gyre. This is primarily dictated by closer proximity to the ice edge and stronger atmo-  
362 spheric forcing there, as the water column is more preconditioned for overturning near the center  
363 of the gyre. Swift and Aagaard (1981) suggested that an inflow of saline Atlantic Water south of  
364 Jan Mayen from the Norwegian Sea could also play a role.

365 The wintertime formation of dense water outside the center of the gyre does not appear to have  
366 a lasting impact on its structure, but could have ramifications on the residence time of this product  
367 and its export from the Iceland Sea. Specifically, dense water located outside the center of the gyre  
368 is more accessible to boundary currents, such as the NIJ, and can therefore more readily supply the  
369 overflows. This is consistent with the low residence time north of the Greenland-Scotland Ridge  
370 estimated for the Arctic-origin overflow water (Smethie Jr. and Swift, 1989).

371 The NIJ provides the densest contribution ( $\sigma_\theta \geq 28.03 \text{ kg/m}^3$ ) to the Denmark Strait overflow  
372 plume and is hypothesized to be part of an interior overturning loop that involves water mass  
373 transformation in the central Iceland Sea (Våge et al., 2011). However, only a minor fraction (2%)  
374 of the 1980 to present late-winter profiles from the north-central Iceland Sea recorded such dense  
375 mixed layers. A lens of weakly stratified water resulting from overturning in winter 2007-2008 was  
376 revealed by an Argo float transiting through the northern Iceland Sea. The lens included waters  
377 denser than  $\sigma_\theta = 28.03 \text{ kg/m}^3$ , implying that this isopycnal had been ventilated that winter even  
378 though direct observations are lacking. Low values of potential vorticity at this deep isopycnal  
379 suggest that water of this density class may be ventilated more often than direct observations of  
380 dense mixed layers indicate. Given a large temporal and spatial variability in convection, it is  
381 likely that the data set used in this study is too sparse to ensure reliable direct detection of the most  
382 intense convective episodes each winter.

383 It is also possible that convection in the Iceland Sea has become less intense over the past two  
384 decades. A deepening of the  $\sigma_\theta = 28.03 \text{ kg/m}^3$  isopycnal in the vicinity of the repeat Langanes  
385 6 station (its location is marked on Fig. 2) may indicate a decrease in the available supply of  
386 the NIJ's densest component. While the only mixed layers denser than  $\sigma_\theta = 28.03 \text{ kg/m}^3$  were  
387 observed in early 2013, the very sparse winter measurements prior to the deployment of Argo  
388 floats in 2005 revealed near-surface waters that had attained similar densities also in early 1981.

389 Swift and Aagaard (1981) found densities in the near-surface layer exceeding  $28 \text{ kg/m}^3$  using  
390 hydrographic data obtained from late February/early March in 1975, and surmised that by the end  
391 of that winter the density could have reached  $28.05 \text{ kg/m}^3$ . Such a decline in the convective activity  
392 was hypothesized by Moore et al. (2015). They documented a trend of diminished wintertime  
393 atmospheric forcing and conducted simulations with a one-dimensional mixed-layer model that  
394 predicted a concomitant reduction in convection. Over time, the result would likely lead to a  
395 weakening of the overturning loop that feeds the NIJ and hence result in a decreased supply of the  
396 densest overflow waters to the AMOC.

397 The time series of winter mean sea to air heat flux and wind stress curl over the north-central  
398 Iceland Sea (Fig. 10) are consistent with this interpretation. Both show a long-term decline that  
399 would lead to a reduction in the buoyancy flux from the ocean to the atmosphere as well as a  
400 reduction in the doming of the isopycnals of the Iceland Sea Gyre. The diminished occurrence  
401 frequency of high heat flux events over the region (Fig. 11) as well as a northward shift in the  
402 location of the heat flux maximum (Fig. 12) contribute to the reduction in the buoyancy flux.  
403 There is evidence of a step-like discontinuity in both the turbulent heat flux and wind stress curl  
404 time series around 1995 that is consistent with the observed long-term behaviour of the depth of  
405 the  $\sigma_\theta = 28.03 \text{ kg/m}^3$  isopycnal (Fig. 7). The timing of these discontinuities are simultaneous  
406 with the transition from NAO positive to NAO neutral conditions (Flatau et al., 2003; Cohen and  
407 Barlow, 2005) that resulted in a number of other changes in the oceanography of the region (e.g.  
408 Häkkinen and Rhines, 2004; Pálsson et al., 2012; Straneo and Heimbach, 2013). However, the  
409 muted dependence of the air-sea forcing over this region on the depth of the Icelandic Low as  
410 compared to the Lofoten Low (Table 1) suggests that further work is required in order to understand  
411 the relative importance of large-scale atmospheric circulation patterns like the NAO and ILD to the  
412 climate of the Nordic Seas.

413 Recent studies have placed a renewed emphasis on the Iceland Sea and strongly suggest that it  
414 provides a more important contribution to the AMOC than previously thought. While the present  
415 hydrographic data set is too sparse to provide a definitive account of the Iceland Sea's recent con-  
416 vective history, in particular as regards its potential to supply the densest component of the NIJ,  
417 there is evidence that also these waters can be locally ventilated. Additional wintertime measure-  
418 ments will continue to shed light on the water mass transformation in the Iceland Sea as a source of  
419 dense water to the NIJ, which will clarify the importance of the Iceland Sea in the North Atlantic  
420 climate system.



## 421 **8. Acknowledgements**

422 The authors would like to thank Bob Pickart for comments to an early version of the manuscript.  
423 Support for this work was provided by the Norwegian Research Council under grant agreement  
424 no. 231647 (KV), the European Union 7th Framework Programme (FP7 2007-2013) under grant  
425 agreement no. 308299 NACLIM Project (KV, SJ, and HV), and the Natural Sciences and Engi-  
426 neering Research Council of Canada (KM).

427 Cohen, J., Barlow, M., 2005. The NAO, the AO, and global warming: How closely related? *Journal*  
428 *of Climate* 18, 4498–4513.

429 Dee, D. P., Uppala, S. M., Simmons, A. J., Berrisford, P., Poli, P., Coauthors, 2011. The ERA-  
430 Interim reanalysis: configuration and performance of the data assimilation system. *Quarterly*  
431 *Journal of the Royal Meteorological Society* 137, 553–597, doi:10.1002/qj.828.

432 Dickson, R. R., Brown, J., 1994. The production of North Atlantic Deep Water: Sources, rates and  
433 pathways. *Journal of Geophysical Research* 99, 12319–12341.

434 Dickson, R. R., Lamb, H. H., Malmberg, S.-A., Colebrook, J. M., 1975. Climatic reversal in  
435 northern North Atlantic. *Nature* 256, 479–482.

436 Eldevik, T., Nilsen, J. E. Ø., Iovino, D., Olsson, K. A., Sandø, A. B., Drange, H., 2009.  
437 Observed sources and variability of Nordic Seas overflow. *Nature Geoscience* 2, 406–410,  
438 doi:10.1038/NGEO518.

439 Flatau, M. K., Talley, L., Niiler, P. P., 2003. The North Atlantic Oscillation, surface current veloc-  
440 ities, and SST changes in the subpolar North Atlantic. *Journal of Climate* 16, 2355–2369.

441 Fogelqvist, E., Blindheim, J., Tanhua, T., Østerhus, S., Buch, E., Rey, F., 2003. Greenland-Scotland  
442 overflow studied by hydro-chemical multivariate analysis. *Deep Sea Research I* 50, 73–102.

443 Gebbie, G., Huybers, P., 2010. Total matrix intercomparison: A method for determining  
444 the geometry of water-mass pathways. *Journal of Physical Oceanography* 40, 1710–1728,  
445 doi:10.1175/2010JPO4272.1.

446 Häkkinen, S., Rhines, P. B., 2004. Decline of subpolar North Atlantic circulation during the 1990s.  
447 *Science* 304, 555–559.

- 448 Hansen, B., Østerhus, S., 2000. North Atlantic–Nordic Seas exchanges. *Progress in Oceanography*  
449 45, 109–208.
- 450 Harden, B. E., Renfrew, I. A., Petersen, G. N., 2011. A climatology of wintertime barrier winds  
451 off southeast Greenland. *Journal of Climate* 24, 4701–4717, doi:10.1175/2011JCLI4113.1.
- 452 Holfort, J., Albrecht, T., 2007. Atmospheric forcing of salinity in the overflow of Denmark Strait.  
453 *Ocean Science* 3, 411–416.
- 454 Hurrell, J. W., 1995. Decadal trends in the North Atlantic Oscillation: Regional temperatures and  
455 precipitation. *Science* 269, 676–679.
- 456 Hurrell, J. W., Deser, C., 2009. North Atlantic climate variability: The role of the North Atlantic  
457 Oscillation. *Journal of Marine Systems* 78, 28–41.
- 458 Jahnke-Bornemann, A., Bruemmer, B., 2009. The Iceland-Lofoten pressure difference: differ-  
459 ent states of the North Atlantic low-pressure zone. *Tellus* 61, 466–475. doi:10.1111/j.1600-  
460 0870.2009.00401.x.
- 461 Jeansson, E., Jutterström, S., Rudels, B., Anderson, L. G., Olsson, K. A., Jones, E. P., Smethie Jr.,  
462 W. M., Swift, J. H., 2008. Sources to the East Greenland Current and its contribution to the Den-  
463 mark Strait Overflow. *Progress in Oceanography* 78, 12–28, doi:10.1016/j.pocean.2007.08.031.
- 464 Jochumsen, K., Quadfasel, D., Valdimarsson, H., Jónsson, S., 2013. Variability of the Denmark  
465 Strait overflow: Moored time series from 1996–2011. *Journal of Geophysical Research* 117,  
466 C12003, doi:10.1029/2012JC008244.
- 467 Jónsson, S., 1992. Sources of fresh water in the Iceland Sea and the mechanisms governing its  
468 interannual variability. *ICES Marine Science Symposia* 195, 62–67.
- 469 Jónsson, S., 1999. The circulation in the northern part of the Denmark Strait and its variability.  
470 *ICES report CM-1999/L:06*, 9 pp.
- 471 Jónsson, S., 2007. Volume flux and fresh water transport associated with the East Icelandic Current.  
472 *Progress in Oceanography* 73, 231–241, doi:10.1016/j.pocean.2006.11.003.
- 473 Jónsson, S., Valdimarsson, H., 2004. A new path for the Denmark Strait overflow wa-  
474 ter from the Iceland Sea to Denmark Strait. *Geophysical Research Letters* 31, L03305,  
475 doi:10.1029/2003GL019214.

- 476 Kelly, P. M., Goodess, C. M., Cherry, B. S. G., 1987. The interpretation of the Icelandic sea ice  
477 record. *Journal of Geophysical Research* 92, 10835–10843.
- 478 Köhl, A., 2010. Variable source regions of Denmark Strait and Faroe Bank Channel overflow  
479 waters. *Tellus* 62A, 551–568, doi:10.1111/j.1600-0870.2010.00454.x.
- 480 Livingston, H. D., Swift, J. H., Östlund, H. G., 1985. Artificial radionuclide tracer supply to the  
481 Denmark Strait overflow between 1972 and 1981. *Journal of Geophysical Research* 90, 6971–  
482 6982.
- 483 Logemann, K., Ólafsson, J., Snorrason, Á., Valdimarsson, H., Marteinsdóttir, G., 2013. The cir-  
484 culation of Icelandic waters - a modelling study. *Ocean Science* 9, 931–955, doi:10.5194/os-9-  
485 931-2013.
- 486 Lorbacher, K., Dommenges, D., Niiler, P. P., Köhl, A., 2006. Ocean mixed layer depth: A sub-  
487 surface proxy of ocean-atmosphere variability. *Journal of Geophysical Research* 111, C07010,  
488 doi:10.1029/2003JC002157.
- 489 Malmberg, S.-A., Jónsson, S., 1997. Timing of deep convection in the Greenland and Iceland Seas.  
490 *ICES Journal of Marine Science* 54, 300–309.
- 491 Marshall, J., Dobson, F., Moore, G., Rhines, P., Visbeck, M., Coauthors, 1998. The Labrador Sea  
492 Deep Convection Experiment. *Bulletin of the American Meteorological Society* 79, 2033–2058.
- 493 Marshall, J., Schott, F., 1999. Open-ocean convection: Observations, theory, and models. *Reviews*  
494 *of Geophysics* 37, 1–64.
- 495 Mauritzen, C., 1996. Production of dense overflow waters feeding the North Atlantic across the  
496 Greenland-Scotland Ridge. Part 1: Evidence for a revised circulation scheme. *Deep Sea Re-*  
497 *search I* 43, 769–806.
- 498 Meincke, J., 1978. On the distribution of low salinity intermediate water around the Faroes.  
499 *Deutsche Hydrographische Zeitschrift* 31, 50–64.
- 500 Meincke, J., 1983. The modern current regime across the Greenland Scotland Ridge. In: Bott, M.  
501 H. P., Saxov, S., Talwani, M., Thiede, J. (Eds.), *Structure and development of the Greenland*  
502 *Scotland Ridge, new methods and concepts*. Plenum Press, pp. 637–650.

- 503 Moore, G. W. K., 2012. Decadal variability and a recent amplification of the summer Beaufort Sea  
504 High. *Geophysical Research Letters* 39, doi:10.1029/2012GL051570.
- 505 Moore, G. W. K., Renfrew, I. A., Pickart, R. S., 2012. Spatial distribution of air-sea heat  
506 fluxes over the sub-polar North Atlantic Ocean. *Geophysical Research Letters* 39, L18806,  
507 doi:10.1029/2012GL053097.
- 508 Moore, G. W. K., Straneo, F., Oltmanns, M., 2014. Trend and inter-annual variability in south-  
509 east Greenland sea ice: impacts on coastal Greenland climate variability. *Geophysical Research*  
510 *Letters*, in press.
- 511 Moore, G. W. K., Våge, K., Pickart, R. S., Renfrew, I. A., 2015. Open-ocean convection becoming  
512 less intense in the Greenland and Iceland Seas. *Nature Climate Change*, submitted for publica-  
513 tion.
- 514 Nilsen, J. E. Ø., Falck, E., 2006. Variations of mixed layer properties in the Norwegian Sea for the  
515 period 1948-1999. *Progress in Oceanography* 70, 58–90, doi:10.1016/j.pocean.2006.03.014.
- 516 Olsson, K. A., Jeansson, E., Tanhua, T., Gascard, J.-C., 2005. The East Greenland Current studied  
517 with CFCs and released sulphur hexafluoride. *Journal of Marine Systems* 55, 77–95.
- 518 Østerhus, S., Sherwin, T., Quadfasel, D., Hansen, B., 2008. The overflow transport east of Iceland.  
519 In: Dickson, R. R., Meincke, J., Rhines, P. (Eds.), *Arctic-Subarctic Ocean Fluxes: Defining the*  
520 *role of the northern seas in climate*. Springer, Dordrecht, The Netherlands, pp. 427–441.
- 521 Pálsson, Ó. K., Gislason, A., Guðfinnsson, H. G., Gunnarsson, B., Ólafsdóttir, S. R., Petursdóttir, H.,  
522 Sveinbjörnsson, S., Thorisson, K., Valdimarsson, H., 2012. Ecosystem structure in the Iceland  
523 Sea and recent changes to the capelin (*Mallotus villosus*) population. *ICES Journal of Marine*  
524 *Science*, doi:10.1093/icesjms/fss071.
- 525 Perkins, H., Hopkins, T. S., Malmberg, S.-A., Poulain, P.-M., Warn-Varnas, A., 1998. Oceano-  
526 graphic conditions east of Iceland. *Journal of Geophysical Research* 103, 21531–21542.
- 527 Pickart, R. S., Torres, D. J., Clarke, R. A., 2002. Hydrography of the Labrador Sea during active  
528 convection. *Journal of Physical Oceanography* 32, 428–457.
- 529 Renfrew, I. A., Moore, G. W. K., 1999. An extreme cold-air outbreak over the Labrador Sea: Roll  
530 vortices and air-sea interaction. *Monthly Weather Review* 127, 2379–2394.

- 531 Renfrew, I. A., Petersen, G. N., Sproson, D. A. J., Moore, G. W. K., Adiwidjaja, H., Zhang, S.,  
532 North, R., 2009. A comparison of aircraft-based surface-layer observations over Denmark Strait  
533 and the Irminger Sea with meteorological analyses and QuikSCAT winds. *Quarterly Journal of*  
534 *the Royal Meteorological Society* 135, 2046–2066, doi: 10.1002/qj.444.
- 535 Rhines, P. B., Häkkinen, S., Josey, S. A., 2008. Is oceanic heat transport significant in the climate  
536 system? In: Dickson, R. R., Meincke, J., Rhines, P. (Eds.), *Arctic-Subarctic Ocean Fluxes:*  
537 *Defining the role of the northern seas in climate.* Springer, Dordrecht, The Netherlands, pp.  
538 87–109.
- 539 Rudels, B., Eriksson, P., Buch, E., Budéus, G., Fahrbach, E., Malmberg, S.-A., Meincke, J.,  
540 Mälkki, P., 2003. Temporal switching between sources of the Denmark Strait overflow water.  
541 *ICES Marine Science Symposia* 219, 319–325.
- 542 Rudels, B., Fahrbach, E., Meincke, J., Budéus, G., Eriksson, P., 2002. The East Greenland Current  
543 and its contribution to the Denmark Strait overflow. *ICES Journal of Marine Science* 59, 1133–  
544 1154.
- 545 Rudnick, D. L., Davis, R. E., 2003. Red noise and regime shifts. *Deep Sea Research I* 50, 691–699.
- 546 Serreze, M. C., Carse, F., Barry, R. G., Rogers, J. C., 1997. Icelandic Low cyclone activity: Clima-  
547 tological features, linkages with the NAO, and relationships with recent changes in the Northern  
548 Hemisphere circulation. *Journal of Climate* 10, 453–464.
- 549 Smethie Jr., W. M., Swift, J. H., 1989. The Tritium:Krypton-85 age of Denmark Strait Overflow  
550 Water and Gibbs Fracture Zone Water just south of the Denmark Strait. *Journal of Geophysical*  
551 *Research* 94, 8265–8275.
- 552 Stefánsson, U., 1962. North Icelandic waters. *Rit Fiskideildar* 3, 1–269.
- 553 Straneo, F., Heimbach, P., 2013. North Atlantic warming and the retreat of Greenland’s outlet  
554 glaciers. *Nature* 504, 36–43, doi:10.1038/nature12854.
- 555 Strong, C., 2012. Atmospheric influence on Arctic marginal ice zone position and width  
556 in the Atlantic sector, February-April 1979-2010. *Climate Dynamics* 39, 3091–3102,  
557 doi:10.1007/s00382-012-1356-6.

- 558 Swift, J. H., Aagaard, K., 1981. Seasonal transitions and water mass formation in the Iceland and  
559 Greenland Seas. *Deep Sea Research* 28A, 1107–1129.
- 560 Swift, J. H., Aagaard, K., Malmberg, S.-A., 1980. The contribution of the Denmark Strait overflow  
561 to the deep North Atlantic. *Deep Sea Research* 27A, 29–42.
- 562 Talley, L. D., McCartney, M. S., 1982. Distribution and circulation of Labrador Sea Water. *Journal*  
563 *of Physical Oceanography* 12, 1189–1205.
- 564 Tanhua, T., Olsson, K. A., Jeansson, E., 2005. Formation of Denmark Strait overflow water and its  
565 hydro-chemical composition. *Journal of Marine Systems* 57, 264–288.
- 566 Tanhua, T., Olsson, K. A., Jeansson, E., 2008. Tracer evidence of the origin and variability of  
567 Denmark Strait Overflow Water. In: Dickson, R. R., Meincke, J., Rhines, P. (Eds.), *Arctic-*  
568 *Subarctic Ocean Fluxes: Defining the role of the northern seas in climate*. Springer, Dordrecht,  
569 The Netherlands, pp. 475–503.
- 570 Våge, K., Pickart, R. S., Spall, M. A., Moore, G. W. K., Valdimarsson, H., Torres, D. J., Erofeeva,  
571 S. Y., Nilsen, J. E. Ø., 2013. Revised circulation scheme north of the Denmark Strait. *Deep Sea*  
572 *Research I* 79, 20–39, doi:10.1016/j.dsr.2013.05.007.
- 573 Våge, K., Pickart, R. S., Spall, M. A., Valdimarsson, H., Jónsson, S., Torres, D. J., Østerhus, S.,  
574 Eldevik, T., 2011. Significant role of the North Icelandic Jet in the formation of Denmark Strait  
575 Overflow Water. *Nature Geoscience* 4, 723–727, doi:10.1038/NGEO1234.
- 576 Våge, K., Pickart, R. S., Thierry, V., Reverdin, G., Lee, C. M., Petrie, B., Agnew, T. A., Wong, A.,  
577 Ribergaard, M. H., 2009. Surprising return of deep convection to the subpolar North Atlantic  
578 Ocean in winter 2007-2008. *Nature Geoscience* 2, 67–72, doi:10.1038/NGEO382.
- 579 Voet, G., Quadfasel, D., Mork, K. A., Sjøiland, H., 2010. The mid-depth circulation of the  
580 Nordic Seas derived from profiling float observations. *Tellus* 62, 516–529, doi:10.1111/j.1600–  
581 0870.2010.00444.x.
- 582 Wernli, H., Schwierz, C., 2006. Surface cyclones in the ERA-40 dataset (1958-2001), part I: Novel  
583 identification method and global climatology. *Journal of the Atmospheric Sciences* 63, 2486–  
584 2507.

- 585 Wong, A. P. S., Johnson, G. C., Owens, W. B., 2003. Delayed-mode calibration of autonomous  
586 CTD float profiling salinity data by  $\theta$ -S climatology. *Journal of Atmospheric and Oceanic Tech-*  
587 *nology* 20, 308–318.
- 588 Yang, J., Pratt, L. J., 2014. Some dynamical constraints on upstream pathways of the Denmark  
589 Strait overflow. *Journal of Physical Oceanography* 44, 3033–3053, doi:10.1175/JPO–D–13–  
590 0227.1.